Charge Transfer Cross Sections of Slow Multiply Charged Neon Ions in Collisions with Noble Gas Atoms*)

Toshio KUSAKABE and Toshizo SHIRAI[1)†]

Kinki University, 3-4-1 Kowakae, Higashi-Osaka 577-8502, Japan

[1)]*Japan Atomic Energy Research Institute, Naka-shi, Ibaraki 319-0193, Japan*

(Received 10 December 2013 / Accepted 1 April 2014)

Single and multiple charge transfer cross sections for Ne^{q+} (q = 2 - 6) ions were measured in collisions with Ne, Ar, Kr, and Xe atoms at $2q$ keV. Quintuple charge transfer cross sections $\sigma_{6,1}$ were derived for the Ne^{6+} + Ne, Ar, and Xe collisions. In Ne atoms, the double, triple, and quadruple charge transfer of Ne^{2+}, Ne^{3+}, and Ne^{4+} ions, respectively, represent so-called symmetric resonant charge transfer processes. The present data for these collisions are in good accordance with the previous data. The scaling properties of the total, single, and multiple charge transfer cross sections were examined, and it was found that the double, triple, and quadruple charge transfer cross sections can be scaled using the second, third, and fourth ionization potentials, respectively.

Keywords: charge transfer cross section, slow multiply charged neon ion, noble gas atom, growth rate method, scaling law, plasma modeling

DOI: 10.1585/pfr.9.3401119

1. Introduction

Fundamental collision data of various atomic processes are indispensable to plasma modeling in fusion science and astrophysics. The accurate knowledge of charge transfer processes and accumulation of charge transfer cross sections between multiply charged ions and neutral particles are critically important in better understanding of low temperature edge plasmas, and their plasma modeling in the fusion devices [1]. In current controlled thermonuclear fusion devices with a gas puffing system, the collisions of inert gas atoms and ions play a key role in cooling and diagnostics of low temperature edge plasmas [1, 2]. In the 1990 s, X-ray emissions from many comets were observed, and the origin of the emissions was attributed to the charge transfer in solar wind ions involving Ne ions from the cometary gases [3].

The first systematic measurements of charge transfer cross sections were performed by Salzborn and coworkers [4–7]. To the best of our knowledge, however, charge transfer cross section measurements of multiply charged Ne ions colliding with noble gas atoms are sparse at low collision energy.

In this study, therefore, we have measured single and multiple charge transfer cross sections $\sigma_{q,q-k}$ of Ne^{q+} ions (q = 2 - 6) in collisions with Ne, Ar, Kr, and Xe atoms at $2q$ keV where q is the incident charge number of primary ions and k is the final number of the charge transferred orbital electrons. Because we observed the final charge states of primary ions passing through the target gas, the "k charge transfer" cross section $\sigma_{q,q-k}$ for the final $(q-k)$+ ions includes both radiative and Auger processes. The total charge transfer cross section σ_{tot} represents the summation of the cross sections for all possible numbers of transferred electrons. The scaling properties of the present single, total, and multiple charge transfer cross sections are also discussed.

2. Experimental

A detailed description of the experimental apparatus and methods used in the present study is reported elsewhere [8–10]. Only the important points and differences are briefly mentioned.

Multiply charged neon ions were produced by a compact electron beam ion source called micro-EBIS [11] using a strong ring permanent magnet. The extracted ions were separated with a Wien filter according to their specific charge (charge/mass). To avoid the contaminations of $^{12}C^{3+}$ and $^{16}O^{4+}$ ions, stable isotope $^{22}Ne^{5+}$ ions were used instead of $^{20}Ne^{5+}$ ions. When Ar atoms were used as the target gas, stable isotope $^{22}Ne^{2-5+}$ ions were used to avoid the contaminations of Ar^{4+}, Ar^{6+}, Ar^{8+}, and Ar^{10+} ions, which are generated when the target gas enters the EBIS. For the same reason, $^{22}Ne^{3+}$ ions were used in the Kr target.

Then, the selected beam of multiply charged Ne ions was introduced into a 40 mm long collision cell filled with target gases of more than 99.9% purity. The target gas pressure in the collision cell was measured with a calibrated high-sensitivity Pirani gauge and ranged from 0.002 to 1 Pa. After the charge transfer collisions, the charged and

† deceased

author's e-mail: kusakabe@phys.kindai.ac.jp

*) This article is based on the presentation at the 23rd International Toki Conference (ITC23).

neutral Ne particles emerging from the cell were separated with an electrostatic deflector and detected with a position-sensitive micro channel plate detector (MCP-PSD). The charge transfer cross sections were determined based on the initial growth rate method, that is, each charge fraction of the product Ne ions and atoms formed in the charge transfer collision was observed against the target gas thickness and was fitted to a quadratic function of the target thickness. The charge transfer cross sections were determined from the slope of the linear part of the observed fraction curves. The detection efficiencies of the present MCP-PSD for Ne^{q+} and neutral Ne particles are assumed to be identical within the experimental uncertainties over the present collision energy range, as discussed in the previous studies [12–14]. The vacuum system was evacuated with two turbo molecular pumps (50 and 500 l/s) and a cryogenic pump. The typical residual gas pressure was approximately 5×10^{-7} Pa in the vacuum chambers containing the micro-EBIS.

The statistical and systematic uncertainties of the observed single and multiple charge transfer cross sections were separately determined. As a result, the total experimental uncertainties of the absolute cross sections are given as the quadratic sum of these uncertainties and range from 10.1% to 54.2%.

3. Results and Discussion

The present experimental cross sections for single and multiple charge transfer of Ne^{q+} ions colliding with Ne, Ar, Kr, and Xe atoms are listed in Table 1 and shown in Fig. 1. For the Ne^{6+} + Ne, Ar, and Xe collisions, quintuple charge transfer cross sections $\sigma_{6,1}$ were derived.

3.1 Overview and single charge transfer cross sections

In Ne atoms, the double, triple, and quadruple charge transfers of Ne^{2+}, Ne^{3+}, and Ne^{4+} ions, respectively, are so-called symmetric resonant charge transfer processes. The present data for these collisions are in good accordance with the data of Kaneko *et al*. [15]. For Ar atoms, the data of Salzborn and coworkers [4, 7] measured at 30 keV are also shown for comparison. Both their $\sigma_{q,q-1}$ data for Ne^{q+} and Ar^{q+} ions are close to the present data. But their double, triple, and quadruple charge transfer cross sections of Ar^{q+} ions are quite larger than the corresponding present cross section values of Ne ions. For Kr and Xe atoms, the data of Ar^{q+} ions measured by Salzborn and coworkers [5–7] at 30 keV are also shown in Fig. 1. In these cases, not only the multiple charge transfer cross sections but also the single charge transfer cross sections are larger than the present values. It is previously pointed out by Kusakabe *et al*. [8] that the cross section data by Salzborn and coworkers have overestimated with the increase in the ionization potential of the target particles.

Kusakabe *et al*. [8] previously measured the cross sections of single charge transfer by 0.286 keV/q Ar^{q+} (q = 2 - 7), Kr^{q+} (q = 2 - 9), and Xe^{q+} (q = 2 - 11) ions colliding with various kinds of atoms and molecules, and presented a best-fit relation as follows:

$$\sigma^{TK}_{q,q-1} = 9.5 \times 10^{-14} \cdot q^{1.3} \cdot I_1^{-2.0} \,[\mathrm{cm}^2], \quad (1)$$

where the first ionization potential I_1 of the target particles is expressed in units of eV. As shown in Fig. 1, this empirical relation, shown by the solid lines, approximates the single charge transfer cross sections.

Table 1 Single and multiple charge transfer cross sections of Ne^{q+} ions colliding with Ne, Ar, Kr, and Xe atoms at $2q$ keV.

k	q	Cross section $\sigma_{q,q-k}$ ($\times 10^{-16}$ cm^2)			
		Ne	Ar	Kr	Xe
1	2	0.613 ± 0.081	4.92 ± 0.61	6.78 ± 0.89	7.39 ± 0.98
	3	3.39 ± 0.35	34.1 ± 4.3	52.1 ± 6.9	68.5 ± 9.1
	4	21.1 ± 2.2	46.2 ± 5.8	58.4 ± 7.9	48.7 ± 6.7
	5	22.0 ± 2.9	46.1 ± 6.3	81.5 ± 11.0	58.5 ± 7.9
	6	13.3 ± 1.9	50.9 ± 7.2	52.7 ± 8.1	55.2 ± 8.1
2	2	2.12 ± 0.28	1.18 ± 0.15	2.09 ± 0.28	1.87 ± 0.25
	3	1.65 ± 0.17	4.50 ± 0.62	4.40 ± 0.60	4.11 ± 0.54
	4	3.05 ± 0.34	4.73 ± 0.59	5.30 ± 0.71	5.24 ± 0.74
	5	2.59 ± 0.28	6.29 ± 0.86	11.5 ± 1.7	12.3 ± 1.7
	6	1.63 ± 0.23	13.0 ± 1.9	18.8 ± 2.8	16.7 ± 2.6
3	3	0.562 ± 0.075	0.329 ± 0.055	0.462 ± 0.078	0.483 ± 0.123
	4	0.62 ± 0.11	1.45 ± 0.23	1.19 ± 0.21	0.898 ± 0.20
	5	1.09 ± 0.16	1.30 ± 0.23	1.76 ± 0.32	1.77 ± 0.31
	6	1.31 ± 0.21	1.16 ± 0.26	2.52 ± 0.50	3.22 ± 0.64
4	4	0.028 ± 0.015	0.137 ± 0.025	0.0918 ± 0.031	0.139 ± 0.024
	5	0.173 ± 0.038	0.139 ± 0.035	0.216 ± 0.068	0.265 ± 0.089
	6	0.334 ± 0.067	0.282 ± 0.056	0.316 ± 0.099	0.479 ± 0.114
5	6	0.030 ±0.011	0.059 ± 0.032	–	0.143 ± 0.078

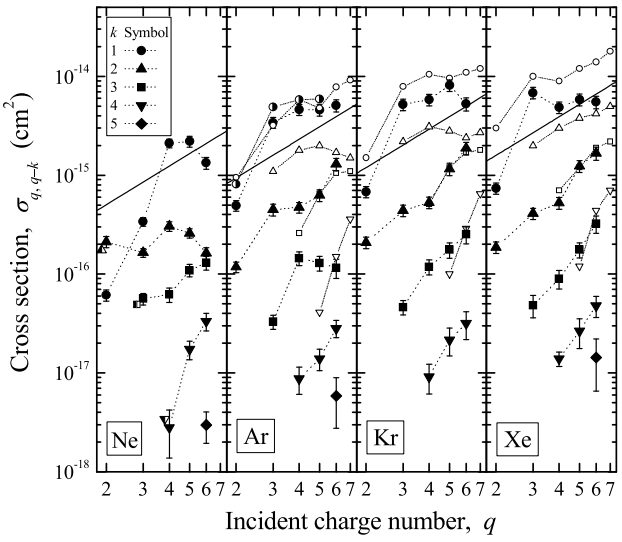

Fig. 1 Single and multiple charge transfer cross sections of Ne^{q+} ions colliding with Ne, Ar, Kr, and Xe atoms. Closed symbols denote the present data. Symbols with left half black are the data of Kaneko *et al*. [15] at $2q$ keV. Circles with right half black and open symbols are the data of Salzborn and coworkers for Ne^{q+} ions [7] and Ar^{q+} ions [4–7] at 30 keV, respectively. Solid lines are the scaling law presented by Kusakabe *et al*. [8]. The dotted lines are drawn for visual aid.

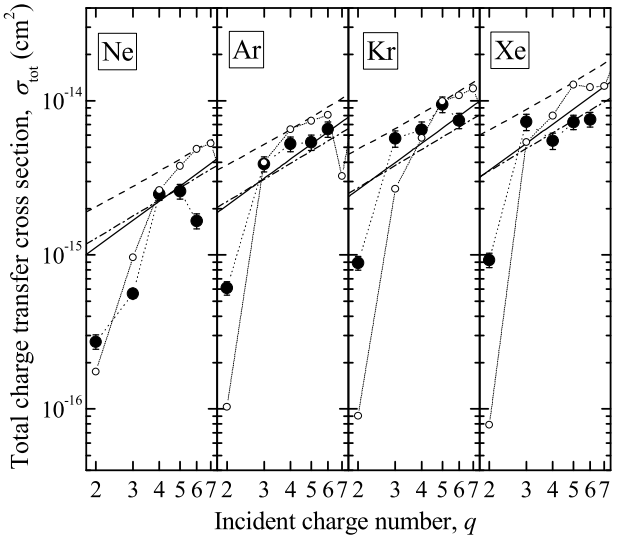

Fig. 2 Total charge transfer cross sections of Ne^{q+} ions colliding with Ne, Ar, Kr, and Xe atoms at $2q$ keV. Solid circles: present data, open circles: EM, dashed curves: CASM [16], dot-dashed lines: TK [21], solid lines: MK [17]. The dotted lines are drawn for visual aid.

3.2 Total charge transfer cross sections

In the framework of the simple classical over-barrier model for a projectile ion with quasi-continuous energy levels, which is called the "classical absorbing sphere model" (CASM) proposed by Janev and Presnyakov [16], one target electron overpasses the potential barrier at a critical internuclear distance R_C. The total charge transfer cross section is given as follows:

$$\sigma_{tot}^{CASM} = \pi R_C^2 = \pi(2\sqrt{q}+1)^2 I_1^{-2}. \quad (2)$$

For $q \gg 1$, the expression σ_{tot}^{CASM} can be approximated as follows:

$$\sigma_{tot}^{MK} = 4\pi q I_1^{-2}. \quad (3)$$

For total charge transfer, this expression is identical to the scaling law proposed by Kimura *et al*. [17].

For an incident ion with discontinuous energy levels, electrons cannot be always transferred even if the over-barrier condition is satisfied. The "energy level matching condition" (EM) has been introduced [18, 19] and the corresponding critical internuclear distance R_C^{EM} is defined as follows:

$$R_C^{EM} = \frac{q-1}{E_B - I_1}, \quad (4)$$

where E_B is the electron binding energy in the $(q-1)$+ ion. Using the value of the actual Ne ion as the E_B values [20], which satisfies the condition $R_C > R_C^{EM}$ and gives the largest R_C^{EM} value, the total charge transfer cross section is expressed as follows:

$$\sigma_{tot}^{EM} = \pi(R_C^{EM})^2. \quad (5)$$

Kusakabe *et al*. [21] previously presented the total charge transfer cross sections for $2q$ keV Ne^{q+} (q = 2 - 6) and Ar^{q+} (q = 2 - 9) ions colliding with various hydrocarbon molecules and the best-fit relation, which is as follows:

$$\sigma_{tot}^{TK} = 1.56 \times 10^{-13} \cdot q^{0.825} \cdot I_1^{-1.75}\ [\mathrm{cm}^2], \quad (6)$$

where I_1 is expressed in units of eV.

In Fig. 2, the observed total charge transfer cross sections are represented by the solid circles. In this figure, the open circles, dashed curves, solid and dot-dashed lines represent the EM, the CASM [16], the scaling law "MK" [17], and the empirical scaling relation "TK" reported by Kusakabe *et al*. [21], respectively. The CASM is believed to give the possible upper limit of the total charge transfer cross sections. The σ_{tot}^{TK} and σ_{tot}^{MK} values are very close. For Ar, Kr, and Xe targets, both σ_{tot}^{TK} and σ_{tot}^{MK} values are close to the present experimental σ_{tot} data, except for $q = 2$. Although the EM results roughly approximate the experimental data, it is not completely in agreement. It is noted that the average rate of the single to total charge transfer cross sections was 79% in the observed collision partners.

3.3 Multiple charge transfer cross sections

Salzborn and coworkers [6, 7] presented the following empirical scaling law for multiple charge transfer cross sections together with the single charge transfer cross sections using the first ionization potential I_1 as follows:

$$\sigma_{q,q-k} = A_k \cdot q^{\alpha_k} \cdot I_1^{-\beta_k}\ [\mathrm{cm}^2], \quad (7)$$

Table 2 Fitting parameters for the present multiple charge transfer cross sections of Ne^{q+} ions colliding with Ne, Ar, Kr, and Xe atoms at $2q$ keV.

k	A_k	α_k	β_k
2	$(1.81 \pm 0.48) \times 10^{-14}$	1.46 ± 0.25	1.70 ± 0.39
3	$(5.0 \pm 1.5) \times 10^{-17}$	2.05 ± 0.30	0.61 ± 0.30
4	$(1.92 \pm 0.38) \times 10^{-18}$	3.79 ± 0.57	0.94 ± 0.38

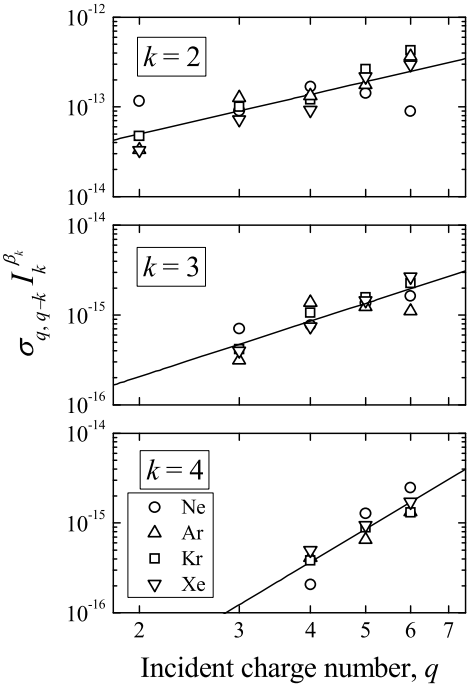

Fig. 3 Reduced plots of the present double, triple, and quadruple charge transfer cross sections against incident charge number q. Experiment: ○, Ne target; Δ, Ar target; □, Kr target; ∇, Xe target. Solid lines denote the best-fit relations $A_k \cdot q^{\alpha_k}$.

where A_k, α_k, and β_k are the fitting parameters. However, as mentioned in the preceding subsection 3.1, multiple charge transfer cross sections measured by Salzborn and coworkers [4–7] are larger than the present values.

Therefore, the fitting parameters A_k, α_k and β_k are re-examined to fit the present multiple charge transfer cross sections by using the k-th ionization potential I_k instead of I_1, and the results are listed in Table 2. In Fig. 3, reduced plots of the present double, triple, and quadruple charge transfer cross sections for Ne^{q+} ions colliding with Ne, Ar, Kr, and Xe atoms are shown as a function of the incident charge number q. Except the data of double charge transfer for the Ne target, the scaling relations fit well with the majority of the present data.

In conclusion, the present observations provide reasonably reliable cross section data for the charge transfer of Ne^{q+} (q = 2 - 6) ions in collisions with Ne, Ar, Kr, and Xe atoms at $2q$ keV. Previously proposed empirical scaling relations approximated the values of the present single and total charge transfer cross sections. For double, triple, and quadruple charge transfer cross sections, new scaling relations are proposed. However, the previous studies of Kr^{2-9+} and Xe^{2-10+} ions [22, 23] have reported that the maximum value in the multiple charge transfer cross section curve appeared with increasing the incident charge number. Further progress of both experimental and theoretical studies is expected to clarify the property of the multiple charge transfer cross sections for highly charged ions.

Acknowledgments

The authors would like to express their sincere appreciation to Doctors Hirotaka Kubo and Tomohide Nakano for valuable discussions. The present study was supported by the Japan Atomic Energy Research Institute.

[1] R.K. Janev, *Atomic and Molecular Processes in Fusion Edge Plasmas* (Plenum, New York, 1995) p.1.
[2] *ITER Physics Basis*, edited by D.W. Ignat, Nucl. Fusion **39**, 2417 (1999).
[3] C.M. Lisse *et al*., Science **274**, 205 (1996).
[4] H .Klinger *et al*., J. Phys. B: At. Mol. Phys. **8**, 230 (1975).
[5] H. Klinger *et al*., J. Chem. Phys. **65**, 3427 (1976).
[6] A. Müller and E. Salzborn, Phys. Lett. **62A**, 391 (1977).
[7] E. Salzborn and A. Müller, *Electronic and Atomic Collisions* (Noth Holland, Amsterdam, 1980) p.407.
[8] T. Kusakabe *et al*., J. Phys. B: At. Mol. Phys. **19**, 2165 (1986).
[9] T. Kusakabe *et al*., J. Phys. Soc. Jpn. **59**, 1218 (1990).
[10] T. Kusakabe *et al*., Plasma Fusion Res. **8**, 2401145 (2013).
[11] T. Kusakabe *et al*., Phys. Scr. **T73**, 378 (1997).
[12] T. Kusakabe *et al*., Phys. Rev. A **68**, 050701(R) (2003).
[13] T. Kusakabe *et al*., Phys. Rev. A **73**, 022706 (2006).
[14] T. Kusakabe *et al*., Plasma Fusion Res. **7**, 2401062 (2012).
[15] Y. Kaneko *et al*., J. Phys. B: At. Mol. Phys. **14**, 881 (1981).
[16] R.K. Janev and L.P. Presnyakov, Phys. Rep. **70**, 1 (1981).
[17] M. Kimura *et al*., J. Phys. B: At. Mol. Opt. Phys. **28**, L643 (1995).
[18] H. Ryufuku *et al*., Phys. Rev. A **21**, 745 (1980).
[19] R. Mann *et al*., J. Phys. B: At. Mol. Phys. **14**, 1161 (1981).
[20] S. Bashkin and J.O. Stoner, Jr., *Atomic Energy Levels and Grotrian Diagrams. 1. Hydrogen I—Phosphorus XV* (North-Holland Pub. Co., Amsterdam, 1975).
[21] T. Kusakabe *et al*., Nucl. Instrum. Methods B **205**, 600 (2003).
[22] T. Kusakabe *et al*., Phys. Scr. **T3**, 191 (1983).
[23] M. Sakisaka *et al*., J. Phys. Soc. Jpn. **52**, 716 (1983).